Water Science & Technology

IWA PUBLISHING

Water Science & Technology Vol 84 No 4, 851 doi: 10.2166/wst.2021.282

Kinetic and thermodynamic studies of polyvinyl chloride composite of manganese oxide nanosheets for the efficient removal of dye from water

Tooba Saeed[a], Abdul Naeem[a,*], Tahira Mahmood[a], Afsar Khan[a], Zahoor Ahmad[a], Muhammad Hamayun[b], Ihtisham Wali Khan[a] and Nazish Huma Khan[c]

[a] National Centre of Excellence in Physical Chemistry, University of Peshawar, Peshawar, Pakistan
[b] Department of Chemistry, University of Gujrat, Gujrat, Pakistan
[c] Department of Environmental Sciences, University of Sawabi, Sawabi, Pakistan
*Corresponding author. E-mail: naeem@uop.edu.pk

ABSTRACT

Manganese oxide nanosheets and manganese oxide composite with polyvinyl chloride (MnO_2-PVC) were synthesized by the oxidation method for the efficient removal of Congo red (CR). The Fourier transform infrared spectroscopy, X-ray diffraction, energy dispersive X-ray, surface area (SA), point of zero charge (PZC) and thermogravimetric analysis were performed to verify the newly synthesized adsorbents. After functionalizing the surface of MnO_2 nanosheets with PVC, the PZC and SA were amplified from 4.10 and 214 $m^2 g^{-1}$ to 5.01 and 226 $m^2 g^{-1}$, respectively. The batch adsorption results showed that the removal capacity of CR on both the adsorbents decreased with the increase of pH and time, but increased with the increase of adsorbent dosage. However, due to the high stability, porosity and greater surface area, the PVC composite of MnO_2 was found to exhibit 15 times greater CR removal efficiency than its parent MnO_2. Furthermore, the thermodynamic parameters specified that CR adsorption onto both the adsorbents was exothermic, spontaneous and film diffusion accompanied by the intraparticle diffusion is the rate controlling step. These results validate that MnO_2 composite with PVC is a useful, eco-friendly, competent candidate for dye removal from wastewater.

Key words: adsorption, Congo red, manganese oxide nanosheets, polyvinyl chloride, thermodynamic study, X-ray diffraction

HIGHLIGHTS

- The current study is competent and environmentally benign for the removal of anionic dye from model aqueous solution.
- The high adsorption capacity of the composite material credited to its unique properties of such as high surface area and porosity.
- The rate controlling step depends on the intra-particle diffusion as well as film diffusion.

GRAPHICAL ABSTRACT

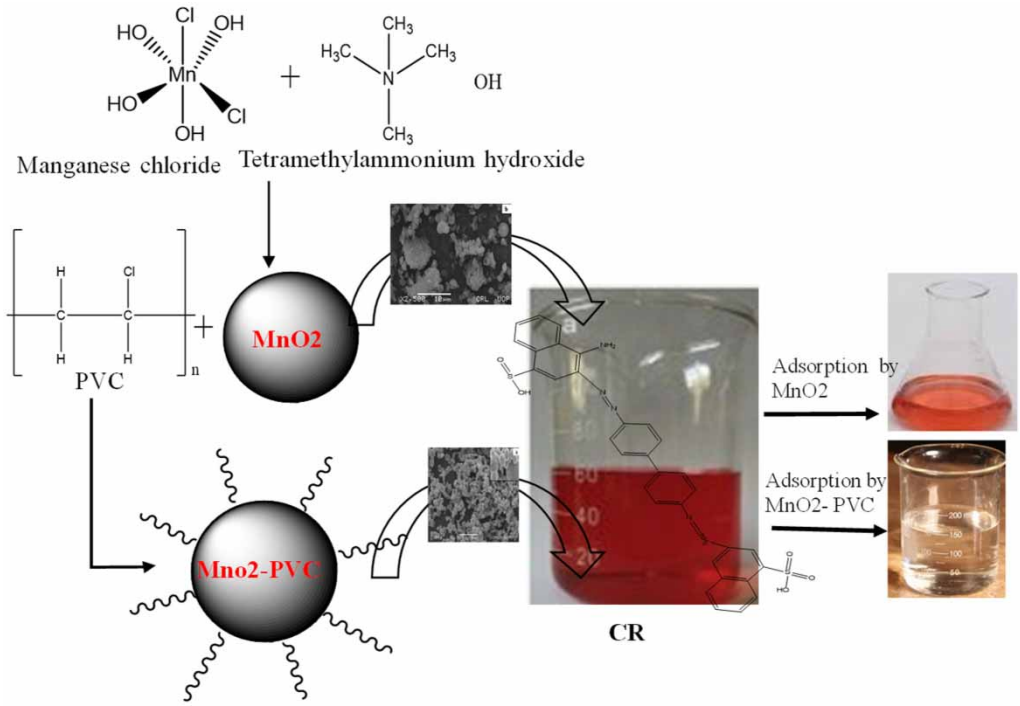

1. INTRODUCTION

Congo red (CR) is an acidic azo dye used as a coloring agent in textile, food, paper, leather and carpet industries (Carolin *et al.* 2017). These industries discharge their effluents directly into water resources (Saeed *et al.* 2020). Dyes are toxic to both human and aquatic organisms and cause respiratory, heart, kidney, lungs, liver, and skin problems. The ingestion of CR ([1-naphthalenesulfonic acid], 3,3′-(4,4′-biphenylenebis) (azo)) metabolizes into benzidine ($C_{12}H_{12}N_2$) which is a cancer-causing agent. Therefore, a proper method for the removal of dyes is needed. Different biological and physio-chemical methods have been discussed in the literature for the removal of dyes (Soltani-Nezhad *et al.* 2020). Among them, adsorption was found to be the attractive one for the removal of dyes from wastewater because it is cheap, fast, eco-friendly and an effective technique (Kumar *et al.* 2014; Fu *et al.* 2020).

However, the choice of a proper adsorbent also plays an important role in the effectual adsorption of dyes. The adsorption capability depends on the properties, type and nature of the adsorbent (Fu *et al.* 2020). Various adsorbents for the removal of CR from wastewater has been reported in the literature. However, among them, the manganese oxide nanosheets and their derivatives have received a reasonable consideration due to their low cost, easy availability, eco-friendliness and innovative properties (Pang *et al.* 2017). Nevertheless, the data regarding the use of polymer composites of metal oxides for the removal of dyes are still very scarce in the literature. A polymer (polyvinyl chloride) is extensively used in electronic cables, clothing, leather stuff and pipes because of its extraordinary properties such as enduring elasticity, repairability, non-toxicity and bioactivity (Landarani *et al.* 2020). The surface modification of manganese oxide nanosheets with polyvinyl chloride (MnO_2- PVC) increased the number of pores, active sites, functional groups and surface area of the parent material (manganese oxide nanosheets), as a result, the adsorption capacity of the material increased (Tang *et al.* 2019; Khan *et al.* 2021). Moreover, PVC also provides stability to the material from leaching and swift dissolution (Wang *et al.* 2021). The possible mechanisms for the surface modification of manganese oxides with polyvinyl chloride include covalent, electrostatic and hydrophobic interactions (Khan *et al.* 2021). However, among them, hydrogen bonding was found to be one of the prevailing mechanisms which can be confirmed from Figure 1(a).

During the course of this investigation, we have proposed innovative, facile, economically viable and efficient adsorbent in the form of polyvinyl chloride composite of manganese oxide nanosheets. The composite is used for the first time for the

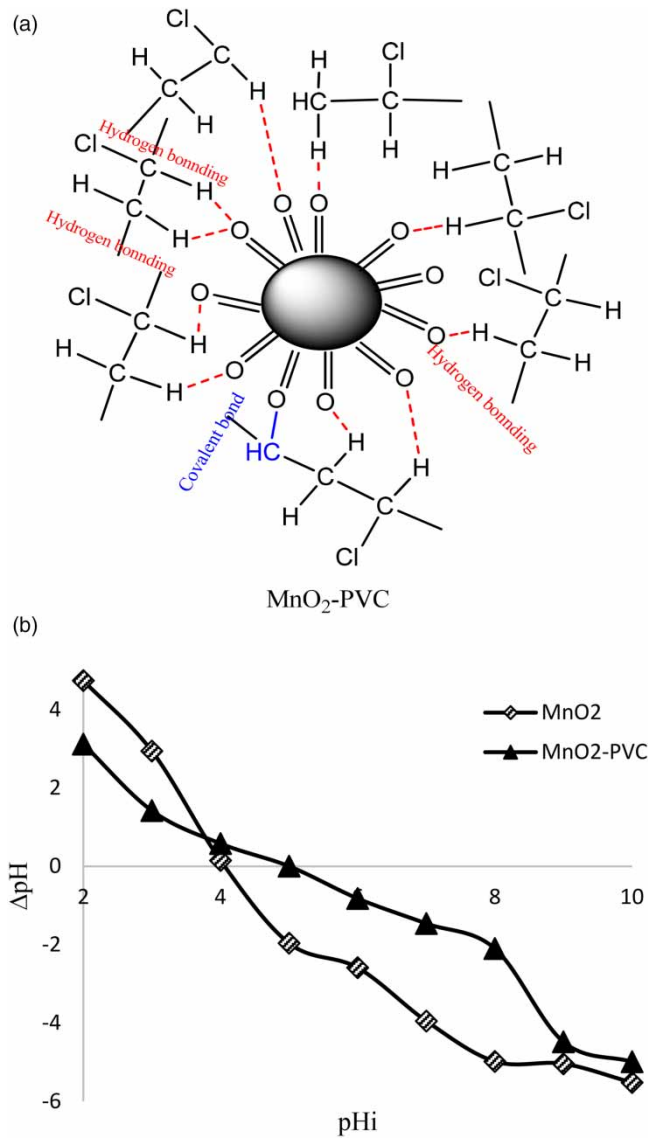

Figure 1 | (a) Interaction between MnO2 and PVC. (b) PZC for MnO_2 nanosheets and MnO_2-PVC composite.

removal of CR from aqueous media. In this study, the elements of the rate-controlling step, spontaneity and the mechanism of CR adsorption onto MnO_2 and MnO_2- PVC were understood by (i) kinetic (ii) thermodynamic and (iii) equilibrium study. Therefore, the main aim of this study is to elucidate the CR removal process through experimental and theoretical studies. On the whole, the combined investigation of theoretical and experimental studies allowed us to achieve new comprehensions for dye removal on verified materials.

2. EXPERIMENTAL

2.1. Chemicals and equipment

During the course of this investigation, deionized water (Millipore) and analytical grade chemicals were used. The chosen dye (CR) was acquired from the manufacturing company Dae-Jung in China. The pH meter (Mettler-Toledo AG, Switzerland) was used for pH measurement. Buffers of pH 3–9 were used for the calibration of the pH meter. To adjust the pH, 0.01–0.5 M solutions of HCl and NaOH obtained from Riedel-de Haen, BDH England were used. Shaker (model BT-150) was used for shaking the dye solutions. The concentration of dye was determined by spectro-VIS spectrometer (Vernier Spectro VIS plus-fluorescence) at their λmax.

2.2. Synthesis of adsorbents

Manganese oxide nanosheets (MnO_2) were synthesized using a hydrothermal method where 1:1 of 0.6 M tetramethylammonium hydroxide (Sigma Aldrich) and 0.3 M manganese chloride tetrahydrate (Sigma Aldrich) mixed within 15 s in 1.5% hydrogen peroxide (Dae-Jung). The resulting mixture was placed for stirring at 25 °C for 2 h and then in an autoclave for 12 h at 100 °C. The resulting slurry was filtered and washed with ethanol (Dae-Jung) as well as deionized water to remove the impurity from the synthesized nanosheets. The resulting solid was then dried in the open air (24 h) and oven for 60 °C (3 h) and 120 °C (24 h) (Peng *et al.* 2017). The dried nanosheets were crushed, ground and stored for further study.

Moreover, the polyvinyl chloride (PVC) composite of manganese oxide nanosheets (MnO_2-PVC) was synthesized by the dropwise mixing of 5 M solution in ethanol of PVC (Dae-Jung) with a 1 M solution of synthesized MnO_2 under continuous stirring. The resulting slurry was decanted 4–6 times, filtered and dried in an oven at 80 °C for 6 h (Li *et al.* 2015). The synthesized MnO_2-PVC was crushed, ground and stored for further study.

2.3. Characterization of adsorbents

The point of zero charge (PZC) was calculated for the synthesized MnO_2 and MnO_2-PVC composite by the method reported by Khan *et al.* (2021). For that, 0.1 g adsorbent was mixed with 0.1 M (40 mL) sodium nitrate solution in different reaction vessels with the initial pH in the range of 2–10. These vessels were placed for 24 h shaking and the final pH of the filtrate was noted. The data were plotted by taking ΔpH versus (vs) initial pH of the solutions.

The surface area of synthesized materials was calculated by quanta-chrome nova 2200e. Whereas the scanning electron microscopy and energy dispersive X-ray patterns were calculated (at 15 kV and 50° inclination) by the models JSM 5910 JEOL and INCA 200. While the Fourier transforms infrared (FTIR) spectroscopy and X-ray diffraction (XRD) patterns were calculated by model Nexus 870 and model JDX-3532, respectively, at room temperature. The vibration frequency of the FTIR patterns was in the range of 500–4,000 cm^{-1}. While the XRD patterns were calculated at 25 mA and 36 kV by manganese filtered Cu-Kα radiations with the λ of 0.15405 nm (in the 2θ range from 5° to 80°). Moreover, the thermogravimetric analyses of both the adsorbents were performed by the thermal analyzer (model NetzschSTA409) in the temperature and airflow range of 0–1,000 °C and 50 mL min^{-1}, respectively. The heating rate used during this technique was 10 °C min^{-1}. The amount of the samples lost was calculated by the furnace (model N71H).

2.4. Adsorption study

Stock solutions of 1,000 (mg L^{-1}) of CR were used for the preparation of working solutions. Batch adsorption experiments were directed to determine the effect of temperature, medium dosage, the concentration of dye, pH and time on the adsorption capability of the MnO_2 and MnO_2–PVC composite. The desired sorbent dosage along with 40 mL of dye solution was taken in a conical flask and was placed in a shaking bath for 3 h at the required pH and temperature. After 3 h, the final pH of the solution was determined and Whatman filter papers 40 were used for filtration. Concentrations of dye before and after sorption was calculated by spectro-VIS spectrometer. The equilibrium concentration (C_e) of dye was calculated with the help of a calibration curve while adsorption capacities (X_e) and percent adsorption of dye were also estimated by Equations (1) and (2) respectively.

$$Xe = \frac{Ci - Ce}{m} \times v \tag{1}$$

$$\%\ removal = \frac{Ci - Ce}{Ci} \times 100 \tag{2}$$

3. RESULTS AND DISCUSSION

3.1. Characterization of MnO_2 nanosheets and MnO_2–PVC composite

3.1.1. Point of zero charge (PZC)

The point of zero charge (PZC) is the pH at which electrical charge compactness is zero. Above that pH_{PZC}, the charge on the surface is negative and, below that, surface is positively charged. According to the data shown in Figure 1(b), the PZC for synthesized MnO_2 nanosheets and MnO_2–PVC composite is found to be 4.10 and 5.01, respectively. A shift in pH_{PZC} value was observed after the contact of polyvinyl chloride (PVC) with the MnO_2, which is similar to the one reported in the literature (El Qada *et al.* 2008).

3.1.2. Surface area analysis (SAA) and scanning electron microscopy (SEM)

The surface areas of MnO_2 and MnO_2-PVC were calculated by the adsorption–desorption method which was found to be 214 and 226 $m^2\ g^{-1}$, respectively. The surface area (SA) of the composite material was found to be higher than the SA of MnO_2 which can be referred to the assimilation of polyvinyl chloride (PVC) onto MnO_2. The PVC, being porous in nature, has increased the functionality and the surface area of the parent material (MnO_2).

The surface morphology and compositional information of the compound are provided by scanning electron microscopy (SEM). The SEM analyses were carried out for the synthesized material using a technique called heat-based treatment where the samples were gathered and electron operating voltage was applied to get the micrographs. The SEM images of MnO_2-PVC and MnO_2 before the adsorption of dye are given in Figure 2(a) and 2(b). These images revealed that the synthesized MnO_2 has a sphere-shape and monodisperse crystals, whereas its surface coverage with the PVC is also clear in the SEM image of MnO_2-PVC (Figure 2(a)).

3.1.3. Energy dispersive X-ray diffraction (EDX)

The elemental analysis of the synthesized materials was determined by energy-dispersive X-ray (EDX). The EDX spectrums of MnO_2 nanosheets and MnO_2–PVC composite before and after adsorption of CR are shown in Figure 3(a)–3(c). It is clear from Figure 3(a) and 3(b) that oxygen and magnesium are the main elements of MnO_2. Whereas, the appearance of additional peaks in the EDX pattern of MnO_2-PVC refers to the presence of carbon and chlorine of polyvinyl chloride. Moreover, in Figure 3(c), the presence of two additional peaks (S and N) strongly supports the adsorption of CR onto MnO_2-PVC.

3.1.4. X-ray diffractometric (XRD) analysis

One of the sophisticated technologies, which is frequently used to define the amorphous, crystalline, or semi-crystalline nature of the sample and also provides an idea about the unit cell dimensions is X-ray diffraction (XRD). The synthesized MnO_2 and MnO_2-PVC were milled into fine particles and their composition was estimated through XRD. The X-ray diffractograms shown in Figure 3(d) reveal that MnO_2 nanosheets are crystalline in nature and the peaks observed are the same as was described by Peng and his research group (Peng *et al.* 2017). Thus, the XRD analysis confirmed the validity of the MnO_2 nanosheets. The assimilation of PVC imparted has no effect on the crystalline nature of MnO_2 nanosheets because the PVC itself is completely amorphous. The results found in the current study are in good agreement with the reported results (Mallakpour *et al.* 2016).

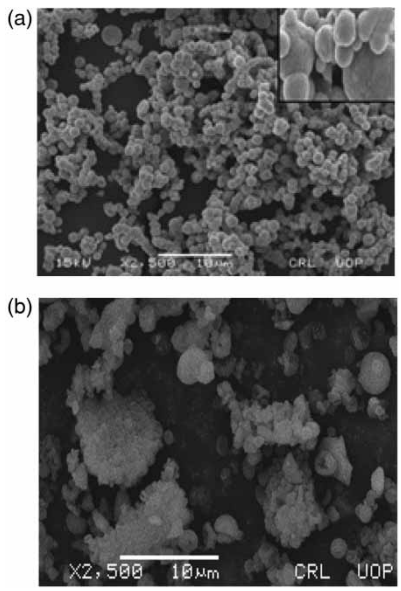

Figure 2 | SEM images of MnO_2-PVC composite (a), SEM image of MnO_2 nanosheets (b).

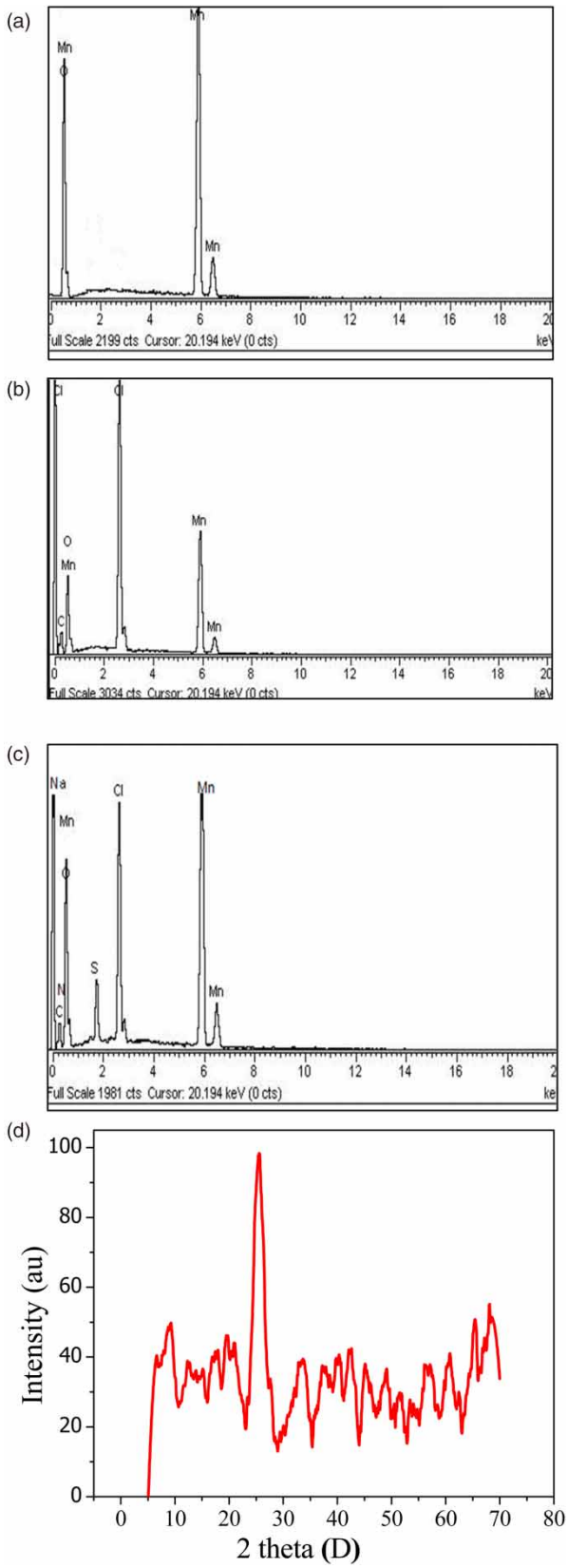

Figure 3 | EDX pattern of MnO_2 nanosheets (a), EDX pattern MnO_2-PVC composite (b), EDX pattern MnO_2-PVC composite after adsorption of CR (c), XRD pattern for MnO_2 nanosheets (d).

3.1.5. Fourier transform infrared (FTIR) spectroscopy

The FTIR study provides information regarding functional groups available at the solid surface. The IR spectra of synthesized MnO_2 nanosheets and MnO_2-PVC composite before and after treating with congo red (CR) are given in Figure 4(a) and 4(b). The appearance of an obvious peak at about 900 cm^{-1} confirms the Mn-O-Mn stretching vibration. Similarly, the band at around 1,034 cm^{-1}, 3,300 cm^{-1} and 3,600 cm^{-1} is assigned to the stretching of the O-H bond with Mn atom as well as the bending and stretching vibration of H-OH molecules. However, the additional peaks appear due to the incorporation of PVC into MnO_2 at about 1,300 cm^{-1}, 1,600 cm^{-1} and 3,000 cm^{-1} referred to as the CH_2-Cl stretching, CH_3 stretching and OH stretching, respectively, which confirmed the formation of PVC composite of MnO_2. Moreover, after CR interaction, the appearance of the peaks at 1,250 cm^{-1} (N-H bending), 1,400 cm^{-1} (C-H bending), 1,700 cm^{-1} (C-N bending) and 2,900 cm^{-1} (O-H stretching) also confirmed the successful adsorption of CR onto both the adsorbents.

3.1.6. Thermo-gravimetric analysis (TGA)

The thermo-gravimetric analysis (TGA) is a thermal technique in which the amount of material is measured at different time intervals with temperature. It tells about the thermal stability of a material. The TGA patterns of MnO_2 nanosheets and MnO_2-PVC composite are shown in Figure 4(c) and 4(d), respectively. In both cases, the first (20–200 °C) and second (200–250 °C) weight loss is attributed to the removal of water and oxygenated molecules. The last weight loss (250–900 °C) in the case of MnO_2 refers to the phase changes in the MnO_2. The third (250–550 °C) and final weight loss (550–1,000 °C) in the case of PVC-MnO_2 composite is credited to the decomposition of the modifier and degradation of the polymer chain present in the composite. However, it is concluded that the inclusively the weight loss in the case of MnO_2-PVC $< MnO_2$ which declared that the composite material is thermally more stable and effective adsorbent for the removal of CR from aqueous media than its counterpart MnO_2.

3.2. Adsorption studies of MnO_2 nanosheets and MnO_2-PVC composite

3.2.1. pH effect

The effect of pH is an important parameter in estimating the adsorption capacity of the synthesized materials and also to probe into the adsorption mechanism. In this connection, the pH effect for the adsorption of CR onto MnO_2 nanosheets and MnO_2-PVC composite was examined by taking 20 mg L^{-1} of CR concentration with optimized experimental conditions. The data shown in Figure 5(a) shows that both the adsorbents exhibit maximum adsorption at the acidic pH values which are lesser than their respective pH_{PZC}. The adsorbents acquire a positive charge at $pH < pH_{PZC}$ due to the greater amount of H^+ ions on their surfaces. Consequently, the positively charged surface attracts the anionic dye from aqueous solutions because of the enhanced electrostatic forces of attraction. Similar findings for the adsorption of dyes were reported elsewhere (Mallakpour *et al.* 2016). Moreover, the affinity of CR towards both the substrates followed the trend MnO_2-PVC $> MnO_2$. This trend reveals that the PVC content is mainly responsible for the higher uptake of the dye onto the MnO_2–PVC composite.

3.2.2. Dosage effect

Being an influential parameter, the effect of the adsorbents ratio on their adsorption capabilities toward CR adsorption was considered in this study. The experimental results of the media dosage on the percent sorption of CR for both MnO_2 and MnO_2-PVC are shown in Figure 5(b). The percent adsorption of MnO_2 and MnO_2-PVC for CR removal was found to increase from 57% to 80% and 92% to 96%, respectively, by increasing the adsorbent amount from 0.01 g to 1.0 g. While the converse is true for the adsorption capacity of both the adsorbents for CR removal (Figure 5(b)). However, an auxiliary increase in dosage was directed to an equilibrium where no further change in adsorption capacity and percent adsorption occurred. The increase in percent adsorption is credited to the increased number of accessible active points on the surfaces of the adsorbents. Whereas, the decrease in the adsorption capacity is due to the incomplete coverage of the adsorption sites. The results observed in the current study are quite similar to the results reported by Liu *et al.* (Hasanzadeh *et al.* 2020) for the adsorption of CR.

3.2.3. Concentration and temperature effect

The dye concentration is likewise vital to conclude the optimum adsorption capacity of the adsorbents. Several adsorption experiments were directed to elucidate the effect of CR concentration onto MnO_2 nanosheets and MnO_2-PVC composite. The study shows that for both the adsorbents, the percent adsorption of dyes was in inverse relation to dye concentrations,

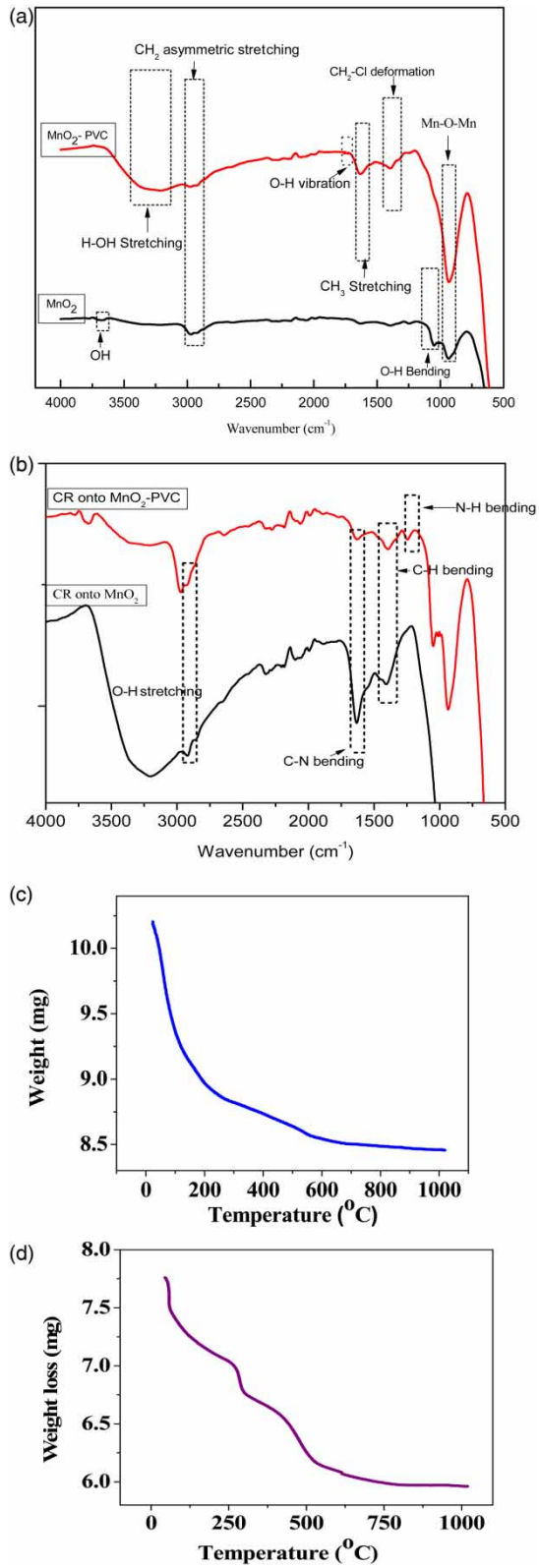

Figure 4 | FTIR pattern of MnO_2 nanosheets, MnO_2-PVC composite before adsorption of CR (a), FTIR pattern of MnO_2 nanosheets, MnO_2-PVC composite after adsorption of CR (b), TGA pattern of MnO_2 nannosheets (c) and TGA pattern of MnO_2-PVC composite (d).

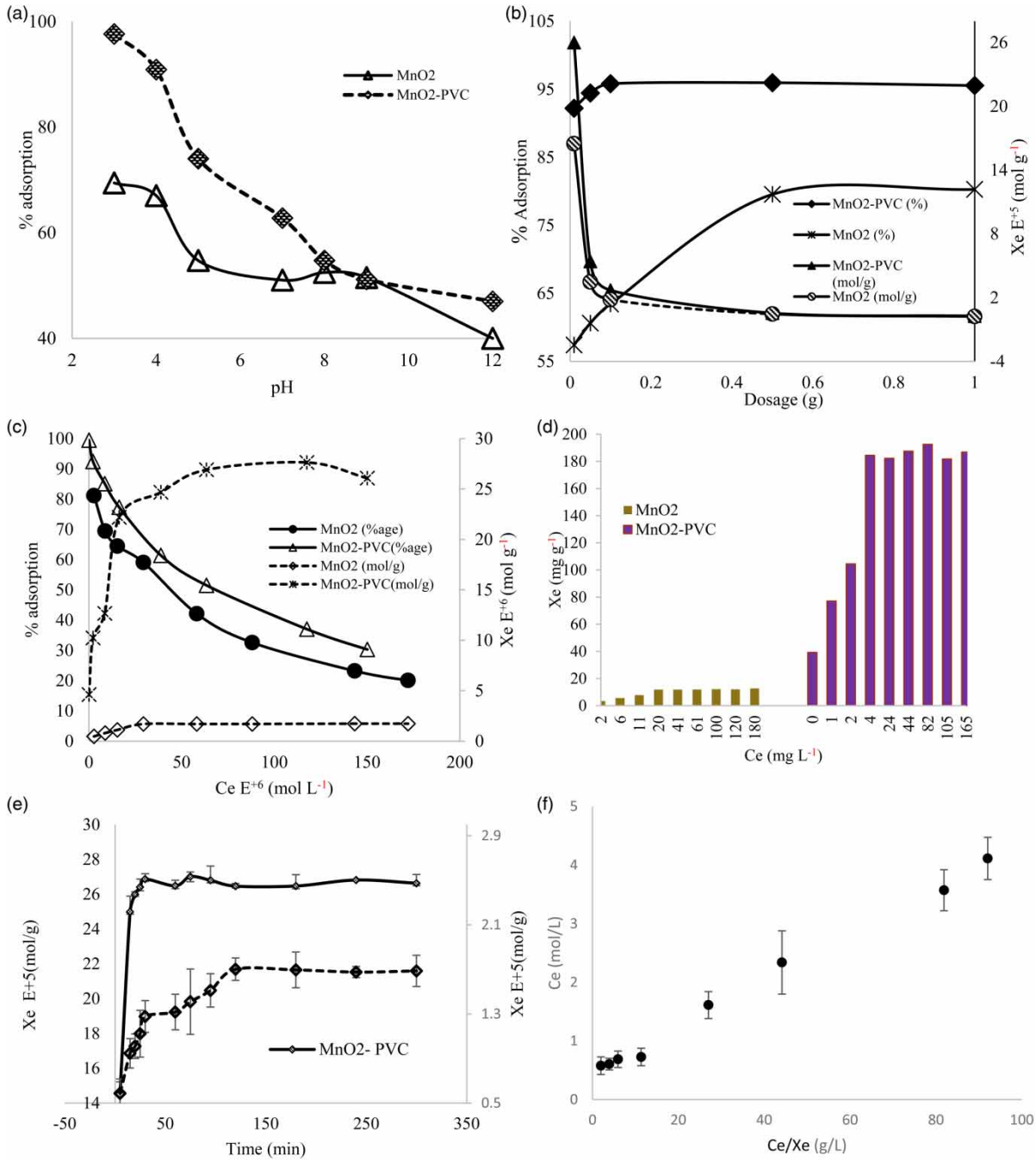

Figure 5 | pH effect of MnO_2 and MnO_2–PVC composite (a), dosage effect of MnO_2 and MnO_2–PVC composite (b), concentration effect of MnO_2 and MnO_2–PVC composite (c), comparative study of MnO_2 and MnO_2–PVC composite (d) and effect of contact time (e) Langmuir adsorption isotherm MnO_2 and MnO_2–PVC composite for CR adsorption (f).

whereas the adsorption capacity was enhanced by the increase of dye concentrations (Figure 5(c)). The data in Figure 5(c) demonstrate that at the very beginning the adsorption of CR on both the adsorbents drastically increases with dye concentration, however, the curves level off and equilibrium in the system is established and no further adsorption occurs with the further increase in the concentration of the dye. The literature revealed that this increase in adsorption capacity is credited to the driving force which is produced by forming the gradient between dye and adsorbent surfaces. The successful adsorption of CR onto both the adsorbents was also confirmed by the FTIR results. The appearance of new peaks in the IR spectra at

1,250 cm^{-1} (N-H bending), 1,400 cm^{-1} (C-H bending), 1,700 cm^{-1} (C-N bending) and 2,900 cm^{-1} (O-H stretching) confirmed the successful adsorption of CR onto both the adsorbents.

The concentration effect on the percent removal of CR onto the MnO2-PVC composite was also examined under different temperatures (298–328 K). It was noticed that the percent adsorption of CR was decreased with the increase of temperature, which is pointing towards the exothermic nature of the process. The adsorption capacity of MnO_2-PVC composite (181 mg g^{-1}) was 15 times greater than that of MnO_2 nanosheets (12 mg g^{-1}) for CR removal (Figure 5(d)). The polyvinyl chloride (PVC) imparts the greater surface area, large pore volume, active sites and stability to MnO_2-PVC which makes it more efficient for the anionic dye removal.

3.3. Kinetic study

The effect of contact time plays a significant role in the removal of CR by MnO_2 nanosheets and MnO_2–PVC composite. The adsorption experiments were undertaken at different time intervals such as 5, 10, 15, 20, 25, 30, 60, 75, and 120 min to determine the equilibrium time for CR removal. It is obvious from Figure 5(e) that the adsorption capacity of CR was sharply increased in the first 15 min and then increased slowly to finally attain the equilibrium. The equilibrium time for CR adsorption was observed to be 120 and 30 min in the case of MnO_2 nanosheets and MnO_2–PVC composite, respectively. The fast adsorption capacity observed during the early stage is credited to the availability of accessible active sites in both cases. However, the minimum equilibrium time for CR adsorption onto MnO_2–PVC composite as compared to MnO_2 is a sign of the industrial importance of MnO_2–PVC composite as it exhibits a greater affinity for the removal of CR from aqueous media. The relatively high adsorption capacity and lower adsorption equilibrium time required for the composite material is not only credited to its greater surface area, but the greater availability of the active sites and functional groups of the composite material is also equally responsible. These characteristics were imparted by the polyvinyl chloride to MnO_2 nanosheets. Kumar *et al.* (2014) also observed a similar trend while studying the dye adsorption onto MnO_2 nanomaterials.

The controlling mechanism and the influence of the equilibrium time for dye uptake from the solution are investigated by different kinetic models. The intraparticle diffusion, Ho's pseudo-second-order, Elovich equation and Lagergren's pseudo-first-order were tested to explain the kinetic data of adsorption. The linear equations of these models are as follows:

$$\ln(Xe - Xt) = \ln Xe - tk_1 \tag{3}$$

$$\frac{t}{Xt} = \frac{1}{k_2 Xe^2} + \frac{t}{Xt} \tag{4}$$

$$Xt = \frac{1}{\beta}\ln(\alpha\beta) + \frac{1}{\beta}\ln t \tag{5}$$

$$Xt = K_{id}t^{0.5} + Ci \tag{6}$$

where Xe and Xt in mol g^{-1} are the equilibrium and adsorption capacities, k_1 (s^{-1}) and k_2 (g mol^{-1} s^{-1}) refer to the pseudo-first and second-order rate constants, Ci (mol g^{-1}) and K_{id} (mol g^{-1} $s^{-0.5}$) are boundary-layer and the intraparticle diffusion parameters and the constants α (mg g^{-1} min^{-1}) and β (g mg^{-1}) are the initial adsorption rate constant and the extent of surface coverage and activation energy for chemisorption.

The most commonly used kinetic model is Lagergren's pseudo-first-order kinetic model. The pseudo-first-order plots were obtained using Equation (3), and from the intercept and slope of the plots, the values of k_1 and X_e were calculated. However, in both the cases, the theoretical values of X_e are different from the experimental ones. It was, therefore, concluded that the adsorption of CR on MnO_2–PVC and MnO_2-PVC composite do not follow pseudo-first-order kinetics. Tang *et al.* (2019) also found that the adsorption mechanism doesn't follow the pseudo-first-order kinetic model while studying the adsorption of anionic dye by silica nanoparticles.

Ho also proposed the pseudo-second-order kinetic model. Using Equation (4), the straight-line graphs were obtained by plotting t/X_t vs. t and the rate constant k_2 and equilibrium concentration X_e were determined from the intercept and slope of the straight line. It is observed from the calculated values that the theoretical values of X_e are closer to the experimental values and also the high values of correlation coefficients were obtained in the case of CR adsorption onto MnO_2 as well as MnO_2–PVC composite. Therefore, it is concluded that the pseudo-second-order kinetic model was strongly followed for the adsorption of CR onto MnO_2 and MnO_2-PVC composite. Liu *et al.* (Hasanzadeh *et al.* 2020) investigated

the CR adsorption onto the modified zeolite and they noted that Ho's kinetic model best explained the CR removal onto zeolite. Similarly, Peng *et al.* (2017) also mentioned that Ho's kinetic model was best applicable to the adsorption of dye onto metal oxide. Moreover, α and β constants of Elovich model are credited to the initial dye removal rate and surface coverage. The calculated factors for all the models are listed in the (Table 1).

Another kinetic model in the form of intraparticle diffusion was applied to explore the rate-determining step of CR removal onto MnO_2 and MnO_2–PVC composite. Equation (6) was used to plot X_t versus $t^{0.5}$ and the values of Ci and K_{id} were calculated from the slope and intercept of the plot (Table 1). Whereas, the intraparticle diffusion and boundary layer constants were obtained from the intercept and slope of the plots. The literature revealed that there may be the possibility of one of the following diffusions:

(i) The boundary layer comprises the adsorption of dye from the dye solution to the boundary layer and surrounds the sorbent. The boundary layer effect depends on the value of Ci where the greater the value of Ci greater will be the boundary layer effect.
(ii) When the dye molecules pass from the boundary to the surface of the sorbent, the resulting diffusion is film diffusion.
(iii) However, the transfer of the molecules from the surface to the intraparticular active sites of the adsorbent gives rise to intraparticle diffusion.

Table 1 | Langmuir, Freundlich, Ho's kinetic model and thermodynamic parameters of CR adsorption onto isotherm model parameters

Ho's Kinetic Model					
Adsorbents	Experimental Xe(mol g^{-1})	Theoretical Xe(mol g^{-1})	k_2 (g mol^{-1} sec^{-1})	R^2	
MnO_2-PVC	2.7 E^{-04}	2.99 E^{-04}	0.76	0.99	
MnO_2	1.77E^{-05}	1.71E^{-05}	0.28	0.99	
Elovich Model					
Adsorbents	α(mg g^{-1} min^{-1})	β(g mg^{-1})	R^2		
MnO_2-PVC	1.9	1.02	0.2		
MnO_2	0.2	5.5	0.8		
Intraparticle Diffusion Model					
Adsorbent	Ci (mol g^{-1})	k_{id} (mol g^{-1} sec^{-1})	R^2		
MnO_2-PVC	0.92	0.33	0.92		
MnO_2	1E^{-06}	1.2E^{-4}	0.99		
Langmuir Isotherm Model					
Adsorbent	Temperature (K)	Kb (L mol^{-1})	Theoretical Xe (mol g^{-1})	Experimental Xe (mol g^{-1})	R^2
MnO_2-PVC	298	11,27,970	2.6 E^{-04}	2.7 E^{-04}	0.99
MnO_2	298	1,20,447	1.71E^{-05}	1.77E^{-05}	0.99
Freundlich Isotherm Model					
Adsorbent	n (g L^{-1})	Kf (mol g^{-1})	R^2		
MnO_2-PVC	3.47	9.48	0.80		
MnO_2	2.52	121.45	0.91		
Thermodynamic Study					
Adsorbent	Temperature	$-\Delta H$ (kJ mol^{-1})	$-\Delta G$ (kJ mol^{-1})	ΔS (J K^{-1} mol^{-1})	
MnO_2-PVC	298 K	0.0073	47.45	134	
	308 K		48.43		
	318 K		49.63		
	328 K		51.56		
MnO_2	298 K	20.424	− 6,646.49	50	
	308 K		− 3,622.31		
	318 K		− 4,512.64		
	328 K		− 4,842.60		

Both film diffusion and intraparticle diffusion are the slowest steps and determine the rate of the reaction. If the plot of X_t versus $t^{0.5}$ is straight, having no intercept and passes by the origin, then it indicates that the rate-controlling step is due to intraparticle diffusion. Whereas, if the plot has an intercept and the straight line does not cross the origin or the straight line shows multilinearity then the intraparticle diffusion along with the film diffusion is responsible for the rate-limiting step. In the present case, the plots (X_t versus $t^{0.5}$) for the adsorption of CR onto MnO_2 nanosheets and MnO_2-PVC composite were neither a straight line, nor crossed by the origin, which confirms that rate is not purely controlled by intraparticle diffusion and it may be involved film diffusion along with intraparticle diffusion to control the process of adsorption. Similar interpretations were described by Iqbal *et al.* (2021) for the removal of CR onto nano-manganese composite (Iqbal *et al.* 2021).

3.4. Adsorption isotherm

For the successful synthesis and designing of the adsorbents, it is vital to know the adsorption capability of the adsorbents. Different models have been frequently used to determine the concentration of dyes at equilibrium. In this study, the Freundlich and Langmuir isotherm models were studied to determine the adsorption mechanism of CR onto the surface of synthesized MnO_2 nanosheets and MnO_2–PVC composite. These models are described below in detail.

3.4.1. Langmuir adsorption isotherm

The batch adsorption data of CR adsorption onto MnO_2 nanosheets and MnO_2–PVC composite were studied by applying the Langmuir model. The Langmuir model can be articulated by Equation (7).

$$\frac{Ce}{X_e} = \frac{1}{X_m Kb} + \frac{Ce}{X_m} \tag{7}$$

where C_e (mol L^{-1}) is the dye concentration at equilibrium, X_m and X_e in mol g^{-1} are maximum and equilibrium adsorption capacities and Kb (L mol^{-1}) is the equilibrium constant. A linear graph using Equation (7) was obtained by plotting C_e/X_e versus C_e for CR adsorption on both the adsorbent. The X_m and Kb values were obtained from the slope and intercept of the linear plot (Figure 5(f)). The correlation coefficient values were obtained to be 0.99 while the calculated and experimental values of X_m were quite identical in both the cases (Table 1) which confirms the best applicability of the Langmuir isotherm for CR adsorption onto MnO_2 nanosheets and MnO_2–PVC composite. As such, it is concluded that the sorption of CR onto MnO_2 and MnO_2–PVC follow the Langmuir isotherm model. Higher values of the binding energy constant (Kb) reflect the strong interaction of CR dye to both the surface (Table 1). The value of Kb in case of MnO_2–PVC composite is almost 9 times greater than its counterpart MnO_2 which also strongly support the greater affinity and stronger interaction of the dye towards the composite material. Similar observations were recorded for the adsorption of dyes onto metal oxides (Khan *et al.* 2021; Wang *et al.* 2021). Jiabin *et al.* (Pang *et al.* 2017) also reported Langmuir isotherm to explain the adsorption mechanism of dye onto manganese oxide.

3.4.2. Freundlich adsorption isotherm

The Freundlich sorption model is one of the sorption models which describe the empirical relation between the solute with the solid adsorbate surface as well as with the liquid of its contact. This isotherm is mostly used for heterogeneous systems to explain the multi-layer sorption. The Freundlich adsorption isotherm is written in the form:

$$\ln Xe = \ln Kf + 1/n(\ln C_e) \tag{8}$$

where X_e (mol g^{-1}) is an equilibrium adsorption capacity, K_f is Freundlich equilibrium constant, C_e (mol L^{-1}) is the concentration of dye at equilibrium whereas, n is the sorption intensity.

The straight-line plot was obtained by plotting ln X_e versus ln C_e. The values of n and Kf were obtained from the slope and intercept of the plot. Based on the poor correlation coefficient, K_f and n values, it is mentioned that the Freundlich adsorption model is not applicable to the removal of CR by MnO_2 and MnO_2–PVC composite (Mallakpour *et al.* 2016). The comparison of the above-mentioned models reveals that the Langmuir adsorption isotherm is a favorable choice to describe the current adsorption data

3.5. Thermodynamic studies

The effect of temperature on the adsorption of anionic dyes (congo red) by MnO_2 nanosheets as well as MnO_2-PVC composite was carried out at 298 K, 308, 318 and 328 K. The adsorption capacity decreased with the increase of temperature in both the cases, which indicate that the CR adsorption by MnO_2, MnO_2-PVC composite is an exothermic process. Moreover, the adsorption selectivity of both the adsorbents towards CR follows the trend MnO_2-PVC>MnO_2 at all temperatures and the reason for preferential uptake of CR by the composite has been described in the previous section.

The following equations were tested to assess the different thermodynamic parameters for CR adsorption on MnO_2 nanosheets and MnO_2-PVC composite.

$$\ln K_c = \frac{\Delta S}{R} - \frac{\Delta H}{RT} \tag{9}$$

$$\Delta G = \Delta H - T\Delta S \tag{10}$$

where T (K) represents temperature, R is the gas constant in J K^{-1} mol^{-1} and K_c is the equilibrium constant. The data were plotted by taking $\ln K_c$ versus 1/T using Equation (9). The values of thermodynamic parameters (Table 1) such as entropy (ΔS) in J K^{-1} mol^{-1}, enthalpy (ΔH) in kJ mol^{-1} and Gibb's free energy (ΔG) in kJ mol^{-1} were calculated using Equations (9) and (10). The calculated negative ΔG values specified the spontaneity of the adsorption process for CR removal onto MnO_2 and MnO_2-PVC composite. Whereas, the increase in ΔG values with the increase of temperature shows the favorability of dye adsorption at lower temperatures. The values of ΔH were also found to be negative, which further validate that the sorption process of dye on both the adsorbents is exothermic. Moreover, the positive values of ΔS show that there was increased disorderliness in the system and also reveal an increment in the degree of freedom of dye (Liu *et al.* 2014). This increased disorderliness in the system is assigned to the dehydration of the dye molecules at the interface. Furthermore, the CR adsorption was thermodynamically controlled by the entropy of the system.

CONCLUSIONS

From the above discussion, it is concluded that the PVC is bonded chemically to MnO_2 in the MnO_2-PVC composite. The adsorption of CR was observed to increase with the decrease in pH and temperature and increase in the dye concentration. The affinity of the CR towards these adsorbents follows the trend MnO_2-PVC > MnO_2. The mechanism of CR adsorption was found to be electrostatic in nature in both the cases. The successful interaction of dye into both the surfaces was also confirmed through FTIR analysis. The high value of the binding energy constant (Kb) in case of MnO_2–PVC composite than its counterpart MnO_2 also strongly support the greater affinity of the dye towards the composite material. Kinetically, both the intraparticle and film diffusion were involved to control the process of CR adsorption by MnO_2 and MnO_2-PVC composite. Furthermore, the CR adsorption was thermodynamically controlled by the entropy of the system. The MnO_2-PVC composite, being versatile in nature, is hereby recommended to be used in different fields of chemistry such as oxidation, catalysis, and electrolysis.

DATA AVAILABILITY STATEMENT

All relevant data are included in the paper or its Supplementary Information.

REFERENCES

Carolin, C. F., Senthil Kumar, P., Saravanan, A., Joshiba, G. J. & Naushad, M. 2017 Efficient techniques for the removal of toxic heavy metals from the aquatic environment. *J. Environ. Chem. Eng.* **5** (6), 2782–2799.

El Qada, E. N., Allen, S. J. & Walker, G. M. 2008 Adsorption of basic dyes from aqueous solution onto activated carbons. *Chem. Eng. J.* **135** (3), 174–184.

Fu, C., Zhang, H., Xia, M., Lei, W. & Wang, F. 2020 The single/co-adsorption characteristics and microscopic adsorption mechanism of biochar-montmorillonite composite adsorbent for pharmaceutical emerging organic contaminant atenolol and lead ions. *Ecotoxicol. Environ. Saf.* **187** (9), 109763.

Hasanzadeh, M., Simchi, A. & Far, H. S. 2020 Nanoporous composites of activated carbon-metal organic frameworks for organic dye adsorption: synthesis, adsorption mechanism and kinetics studies. *J. Ind. Eng. Chem.* **81** (3), 405–414.

Iqbal, J., Shah, N. S., Sayed, M., Niazi, N. K., Imran, M., Khan, J. A., Khan, Z. U. H., Hussien, A. G. S., Polychronopoulou, K. & Howari, F. 2021 Nano-zerovalent manganese/biochar composite for the adsorptive and oxidative removal of Congo-red dye from aqueous solutions. *J. Hazard. Mater.* **403** (1), 123854.

Khan, F., Naeem, A., Ud Din, I., Saeed, T., Alotaibi, M. A., Alharthi, A. I., Habib, A. & Malik, T. 2021 Synthesis, characterization and adsorption studies of h-BN crystal for efficient removal of Cd2+ from aqueous solution. *Ceram. Int.* **3** (6), 659–672.

Kumar, B. M. P., Shivaprasad, K. H., Raveendra, R. S., Hari Krishna, R., Karikkat, S. & Nagabhushana, B. M. 2014 Preparation of MnO_2 nanoparticles for the adsorption of environmentally hazardous malachite green dye. *Int. J. Appl. or Innov. Eng. Manage.* **3** (12), 102–106.

Landarani, M., Chamjangali, M. A. & Bahramian, B. 2020 Preparation and characterization of a novel chemically modified PVC adsorbent for methyl orange removal: optimization, and study of isotherm, kinetics, and thermodynamics of adsorption process. *Water, Air, Soil Pollut.* **10** (2), 1–17.

Li, Y., Wang, Z., Huang, B., Dai, Y., Zhang, X. & Qin, X. 2015 Synthesis of BiOBr-PVP hybrids with enhanced adsorption-photocatalytic properties. *Appl. Surf. Sci.* **347** (3), 258–264.

Liu, S., Ding, Y., Li, P., Diao, K., Tan, X., Lei, F., Zhan, Y., Li, Q., Huang, B. & Huang, Z. 2014 Adsorption of the anionic dye Congo red from aqueous solution onto natural zeolites modified with N,N-dimethyl dehydroabietylamine oxide. *Chem. Eng. J.* **248** (1), 135–144.

Mallakpour, S., Abdolmaleki, A. & Tabebordbar, H. 2016 Production of PVC/α-MnO2-KH550 nanocomposite films: morphology, thermal, mechanical and Pb (II) adsorption properties. *Eur. Polym. J.* **78** (1), 141–152.

Pang, J., Fu, F., Ding, Z., Lu, J., Li, N. & Tang, B. 2017 Adsorption behaviors of methylene blue from aqueous solution on mesoporous birnessite. *J. Taiwan Inst. Chem. Eng.* **77** (3), 168–176.

Peng, L., Liu, B., Zeng, Q., Gu, J.-D., Lei, M., Shao, J. & Chai, L. 2017 Highly efficient removal of methylene blue from aqueous solution by a novel fishing-net effect of manganese oxide nano-sheets. *Clean Technol. Environ. Policy* **19** (1), 269–277.

Saeed, T., Naeem, A., Ud Din, I., Alotaibi, M. A., Alharthi, A. I., Khan, I. W., Khan, N. H. & Malik, T. 2020 Structure, nomenclature and viable synthesis of micro/nanoscale metal-organic frameworks and their remarkable applications in adsorption of organic pollutants. *Micro. J.* In press, **55** (6), 105579.

Soltani-Nezhad, F., Saljooqi, A., Mostafavi, A. & Shamspur, T. 2020 Synthesis of Fe3O4/CdS–ZnS nanostructure and its application for photocatalytic degradation of chlorpyrifos pesticide and brilliant Green dye from aqueous solutions. *Ecotoxicol. Environ. Saf.* **189** (51), 109886.

Tang, Y., Li, M., Mu, C., Zhou, J. & Shi, B. 2019 Ultrafast and efficient removal of anionic dyes from wastewater by polyethyleneimine-modified silica nanoparticles. *Chemosphere* **229** (8), 570–579.

Wang, Z., Park, H. N. & Won, S. W. 2021 Adsorption and desorption properties of polyethylenimine/polyvinyl chloride cross-linked fiber for the treatment of azo dye reactive yellow 2. *Molecules* **26** (5), 1519.

First received 31 January 2021; accepted in revised form 3 July 2021. Available online 16 July 2021